

Block of Inferior Olive Gap Junctional Coupling Decreases Purkinje Cell Complex Spike Synchrony and Rhythmicity

Timothy A. Blenkinsop and Eric J. Lang

Department of Physiology and Neuroscience, School of Medicine, New York University, New York, New York 10016

Inferior olivary (IO) neurons are electrotonically coupled by gap junctions. This coupling is thought to underlie synchronous complex spike (CS) activity generated by the olivocerebellar system in Purkinje cells, and also has been hypothesized to be necessary for IO neurons to generate spontaneous oscillatory activity. These characteristics of olivocerebellar activity have been proposed to be central to the role of this system in motor coordination. However, the relationship of gap junction coupling between IO neurons to synchronous and rhythmic CS activity has never been directly tested. Thus, to address this issue, multiple electrode recordings were obtained from crus 2a Purkinje cells, and carbenoxolone, a gap junction blocker, was injected into the IO. Carbenoxolone reduced CS synchrony by 50% overall, but in some experiments, >80% reductions were achieved. Carbenoxolone also reduced the average firing rate by 50%, suggesting that electrical coupling is a significant source of excitation for IO neurons. Moreover, carbenoxolone caused a reduction in the ~10 Hz rhythmicity of CS activity, and this reduction was correlated with the extent to which the injection reduced CS synchrony. Lastly, carbenoxolone was found to reverse or prevent changes in synchrony that are normally induced by injection of GABA_A and glutamate receptor antagonists into the IO, suggesting that the effects of these drugs on CS synchrony patterns require electrical coupling of IO neurons. In sum, our results provide direct evidence that electrical coupling of IO neurons underlies synchronous CS activity, and suggest important roles for this coupling in shaping other aspects of IO spiking patterns.

Key words: oscillation; cerebellum; connexin; multielectrode; carbenoxolone; rat

Introduction

Synchronization of Purkinje cell complex spike (CS) activity was proposed to result from electrotonic coupling of inferior olivary (IO) neurons by gap junctions >30 years ago (Llinás, 1974; Llinás et al., 1974). Consistent with this proposal, electrical coupling of IO neurons has been demonstrated using *in vitro* preparations (Llinás and Yarom, 1981a, 1986; Benardo and Foster, 1986; Devor and Yarom, 2002; Long et al., 2002); the IO has a high density of neuronal gap junctions (Sotelo et al., 1974; De Zeeuw et al., 1989); and the IO has one of the highest levels of expression in the CNS of connexin36, the main connexin involved in formation of neuronal gap junctions (Condorelli et al., 1998; Belluardo et al., 2000).

The validity of this evidence with regard to the role of gap junctions in generating CS synchrony rests on the premise that electrical coupling can lead to synchronized spike activity in IO neurons, which in turn would evoke CSs; however, there is reason to question this premise. For example, *in vitro* studies have found relatively low coupling coefficients between IO neurons, which are not sufficient for spike propagation between IO neurons un-

der normal conditions (Manor et al., 2000; Devor and Yarom, 2002).

As an alternative to underlying spike transmission, IO gap junctions were proposed to allow synchronization of subthreshold oscillations in membrane potential that IO neurons display *in vitro* (Lampl and Yarom, 1997; Manor et al., 1997, 2000). Consistent with this idea, connexin36 knock-out mice have greatly reduced electrical coupling between IO neurons, and subthreshold oscillations are not synchronized across cells in these mice (Long et al., 2002). Thus, gap junctions may allow the setting up of a standing wave across all or part of the IO, with CS synchrony then presumably arising from the interaction of synaptic input with the coherent excitability changes in IO neurons resulting from the oscillations.

Several objections may be raised to this mechanism as well. Synchronous CS activity remains after block of major synaptic input to the IO, suggesting IO afferent activity is in fact not needed (Lang et al., 1996; Lang, 2001, 2002); subthreshold oscillations have never been reported *in vivo* (Crill and Kennedy, 1967; Crill, 1970; Llinás et al., 1974; Ruigrok and De Zeeuw, 1993; Ruigrok and Voogd, 1995); and autocorrelograms of rhythmic CS activity are not consistent with it arising from subthreshold oscillations (E. J. Lang, unpublished observations).

These points raise significant questions about how and whether gap junction coupling underlies CS synchrony, and underscore the need for a direct demonstration that CS synchrony is mediated by gap junction coupling of IO neurons. Thus, the effects of intra-IO injections of the gap junction blocker carben-

Received Aug. 30, 2005; revised Dec. 8, 2005; accepted Dec. 15, 2005.

This work was supported by National Institutes of Health—National Institute of Neurological Disorders and Stroke Grant NS37028. We thank D. Paré and S. P. Marshall for comments on a previous draft of this manuscript.

Correspondence should be addressed to Dr. Eric J. Lang, Department of Physiology and Neuroscience, School of Medicine, New York University, 550 First Avenue, New York, NY 10016. E-mail: Lange01@med.nyu.edu.

DOI:10.1523/JNEUROSCI.3677-05.2006

Copyright © 2006 Society for Neuroscience 0270-6474/06/261739-10\$15.00/0

oxolone on CS activity were investigated. Carbenoxolone blocks dye coupling of IO neurons but does not affect non-gap junction conductances of these cells (Leznik and Llinás, 2003; Leznik, 2004; Placantonakis et al., 2004). Thus, changes in CS activity caused by carbenoxolone should reflect changes in the level of IO gap junction coupling and provide answers regarding the role of gap junctions in determining CS activity patterns.

Materials and Methods

Experiments were performed in accordance with the National Institutes of Health's *Guide for the Care and Use of Laboratory Animals*. Experimental protocols were approved by the Institutional Animal Care and Use Committee of New York University School of Medicine.

General surgical procedures and implantation of multiple electrode array. Sprague Dawley rats (225–300 g) were anesthetized with an intraperitoneal injection of ketamine (100 mg/kg) and xylazine (8 mg/kg). Supplemental anesthesia (ketamine, ~6 μ g/kg/min; xylazine, ~1 μ g/kg/min) was given as a continuous infusion via a femoral vein catheter starting ~2 h after the initial dose. The rate of supplemental anesthesia was calibrated to prevent spontaneous and reflex movements and then kept constant throughout the recording sessions. Rectal temperature was maintained at 36–37°C by an electric heating pad. Animals were mechanically ventilated and given supplemental oxygen when necessary.

Following anesthetization, insertion of a femoral catheter, and tracheotomy, the head of the animal was fixed in a stereotaxic apparatus. The cerebellar cortex was exposed by removal of the overlying bone and dura mater and then covered by a platform that was cemented in place over crus 2a. The platform consisted of an electron microscope grid embedded in silicone rubber and fixed to tungsten metal rods with epoxy, and served to hold the microelectrodes in place and guide their spacing.

Microelectrodes consisted of glass pipette tips (3 mm long; 1–3 M Ω) filled with a NaCl/glycerol solution. A platinum–iridium wire was inserted into the base of the tip to connect it to the amplifier system. Microelectrodes were implanted into the cerebellar cortex using a joystick-controlled piezoelectric micromanipulator (EXFO Burleigh Products Group, Victor, NY). Each microelectrode was attached to the micromanipulator via a wax droplet and then pushed through a silicone rubber-filled hole in the grid and down ~100 μ m into the molecular layer of the cerebellum until CS activity was isolated (Fig. 1A). The electrode was then released by melting the wax, and the next electrode was attached to the holder and similarly implanted. This process continued until a 4 \times 10 array of electrodes with an interelectrode spacing of 250 μ m had been implanted into a ~1.7 mm² area of crus 2a (Fig. 1B).

Multielectrode recording system and data acquisition. The multielectrode recording system (MultiChannel Systems, Reutlingen, Germany) consisted of 128 amplifier channels (total gain, 1000 \times) with bandpass filters of 200 Hz to 8 kHz. Data were recorded onto a dual processor personal computer using MultiChannel Systems MCRack data acquisition software (sampling rate, 10–25 kHz/channel). This software allowed a voltage threshold to be set for each channel, the crossing of which was detected as an event. Thresholds were set so as to detect the initial deflection of the CS waveform. On detection of a threshold crossing, the system recorded the time and waveform of the voltage record, which were then used for subsequent off-line spike sorting and data analysis.

The MCRack software had oscilloscope and spike event displays for monitoring activity. The latter display comprised a grid onto which was mapped the electrode array such that each box in the grid corresponded

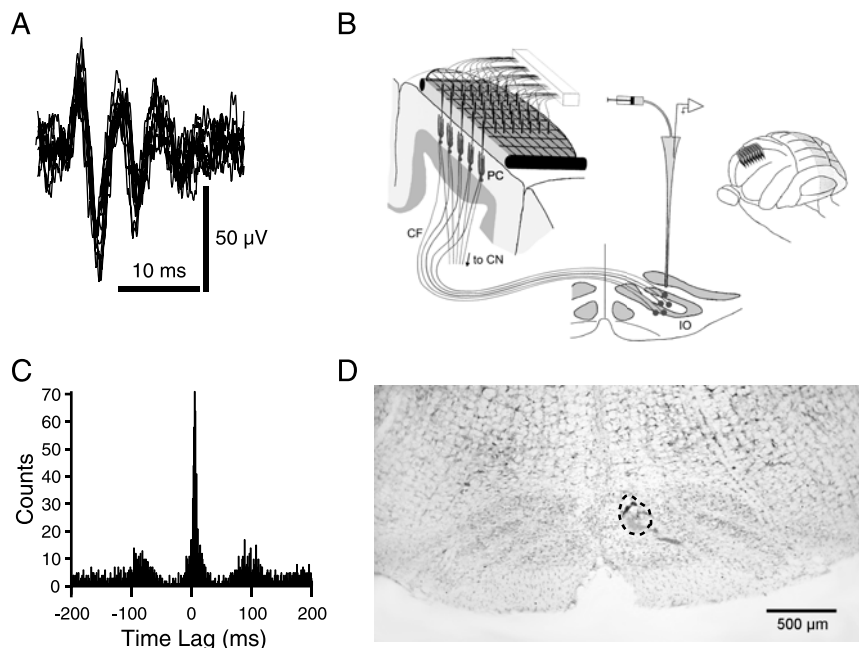


Figure 1. Experimental design and characteristics of spontaneous Purkinje cell CS activity. **A**, Overlaid traces of extracellularly recorded CS activity from one Purkinje cell. **B**, Schematic of the experimental setup showing implantation of electrodes through an electron microscope grid and into the molecular layer of the cerebellar cortex. A pipette is inserted into the contralateral IO to make local injections. Inset shows the approximate location of electrode array on crus 2a. **C**, IO–CS cross-correlogram. Spikes from IO single unit served as the reference for generating correlogram. CSs recorded from one cell in the crus 2a recording array. **D**, Cresyl violet-stained coronal section of the brainstem. Injection location within medial IO is marked by alcian blue dye that was injected at the end of the experiment. The injection site is encircled by a dashed line. CF, Climbing fiber; PC, Purkinje cell; CN, cerebellar nuclei.

to the relative location of the electrode in the brain. A box would flash when the voltage threshold in the corresponding channel was crossed, and thus provided a means for simultaneously monitoring the spike activity from all cells.

Recording sessions were initiated once the voltage thresholds for all channels were set. A control period of 20 or more minutes of spontaneous CS activity was recorded first. This period was followed by recordings of spontaneous CS activity after the various intra-IO drug injections that were performed. In experiments in which stimulus-evoked CSs were recorded, these sessions were interspersed with ones in which spontaneous CS activity was recorded.

Microinjection technique. Intra-IO injections were made using a pipette (tip diameter, 20–30 μ m). To determine the correct injection site, a microelectrode was used to locate IO cells whose activity was strongly correlated with crus 2a CS activity (Fig. 1C) (i.e., correlograms of IO and CS activity with a sharp peak that was offset by 4–5 ms from the histogram center, reflecting the conduction time of the olivocerebellar pathway). The microelectrode was then removed and the pipette inserted to the same coordinates. Pressure injections of drug solutions were made with a syringe pump (CMA Microdialysis, North Chelmsford, MA) at a rate of 0.025 μ l/min, as Ringer's injections at similar rates do not alter CS activity (Lang et al., 1996; Lang, 2001). All drugs were dissolved in a Ringer's solution containing the following (in mM): 126 NaCl, 26 NaHCO₃, 3 KCl, 1.2 KH₂PO₄, 1.6 MgSO₄, 2 CaCl₂, 5 HEPES, and 15 dextrose, pH 7.4. Aside from the dose–response experiments, drug concentrations were as follows: carbenoxolone, 500 μ M; 1,2,3,4-tetrahydro-6-nitro-2,3-dioxo-benzo[f]quinoxaline-7-sulfonamide disodium (NBQX), 200 μ M; and picrotoxin, 2 mg/ml. Drugs were obtained from Sigma (St. Louis, MO). For carbenoxolone, *in vitro* studies have shown that bath concentrations of 100–200 μ M are required to achieve maximal blockade between IO neurons (Leznik, 2004; Placantonakis et al., 2004). We typically used a somewhat higher pipette concentration of 500 μ M, because we were delivering the drug from a point source from which there would be a concentration gradient. Other drug concentrations

were chosen based on previous results showing the efficacy of these values (Lang et al., 1996; Lang, 2001, 2002).

At the conclusion of the recordings, the drug solution was replaced by one containing alcian blue dye while keeping the pipette in place. A small quantity of dye was then injected to mark the pipette location for histological verification (Fig. 1D).

Stimulation techniques. Bipolar electrodes made from tungsten wire were used to apply electrical stimuli (100–200 μ s pulses of 50–500 μ A) to the motor cortex, and/or the cerebellar white matter. Motor cortex electrodes were inserted \sim 1–1.5 mm below the cortical surface in experiments in which NBQX was injected into the IO. The loss of the motor cortex-evoked CS activity was used to verify the efficacy of the injection.

Stimulation of the cerebellar white matter was used to evoke the climbing fiber reflex (Eccles et al., 1966), which was used as a measure of gap junction coupling of IO cells. A stimulus electrode was inserted via crus 1 into the cerebellar white matter to a depth of 1–2 mm. Stimuli (100–200 μ s pulses of 50–500 μ A) were used to elicit climbing fiber reflex responses.

Off-line data analysis. All data analyses were performed within IGOR (WaveMetrics, Lake Oswego, OR) using procedures developed by one of the authors. For each cell, a template matching routine was used to select the spikes from the recorded waveforms.

Calculation of CS synchrony and rhythmicity. To measure the relationship of activity in two different cells, a cross-correlation function was calculated as follows. The spike train of a cell was represented by $X(i)$, where i represents the time step ($i = 1, 2, \dots, N$). $X(i) = 1$ if the CS onset occurs in the i time bin; otherwise, $X(i) = 0$. $Y(i)$ was the same as $X(i)$, but for the reference cell. The cross-correlation coefficient, $C(t)$, was then calculated as follows:

$$C(t) = \frac{\sum_{i=1}^N \{V(i)W(i-t)\}}{\sqrt{\sum_{i=1}^N V(i)^2 \sum_{i=1}^N W(i)^2}}$$

$$V(i) = X(i) - \sum_{j=1}^N X(j)/N, \quad W(i) = Y(i) - \sum_{j=1}^N Y(j)/N,$$

where $V(i)$ and $W(i)$ are the normalized forms of $X(i)$ and $Y(i)$, respectively. A 1 ms time step was used, and thus for two spikes to be considered synchronous, their onsets must occur in the same 1 ms bin. The zero-time cross-correlation coefficient, $C(0)$, was defined as the degree of synchrony between two cells.

To assess CS rhythmicity normalized autocorrelograms were computed for individual cells using the above formula for $C(t)$, with X and Y both representing the same spike train. A 5 ms time step was used. Thus, the autocorrelogram values could range between 1 and -1 , with the central peak always equal to 1. These individual cell autocorrelograms were averaged to obtain population autocorrelograms.

Statistical tests. Unless otherwise specified, mean values are given with their SD. Student's t test, paired or unpaired as appropriate, was used for comparison of population means. For testing whether a correlation coefficient (Pearson's r) was statistically different from zero, r was first converted to Fisher's z' ($z' = 0.5[\ln(1+r) - \ln(1-r)]$), because r is not normally distributed, whereas z' is normally distributed with a SE ($SE_{z'}$) of $1/(n-3)^{1/2}$ (Snedecor and Cochran, 1989). A z -score was then computed as $(z' - 0)/SE_{z'}$ and used to obtain the two-tailed p value.

Histology. Histological controls were obtained to confirm the locations of the injection pipette. At the conclusion of the experiment, the animal was perfused with saline followed by 10% formalin. The brain was removed, soaked in 10% formalin for 1–2 d, and then transferred to a 30% sucrose/10% formalin solution until it sank. Transverse 60 μ m cross sections of the brainstem were prepared on a freezing microtome and mounted on chrome–alum gelatin-coated slides for counterstaining with cresyl violet.

Results

Intra-IO injection of carbenoxolone blocks the climbing fiber reflex

The major aim of this study was to determine the effect of blocking IO gap junctions on spontaneous CS activity using intra-IO injections of carbenoxolone in combination with multiple electrode recording of CSs. However, although this drug has been shown to block dye coupling between IO neurons *in vitro* (Leznik and Llinás, 2003; Leznik, 2004; Placantonakis et al., 2004), its efficacy in blocking electrical coupling under *in vivo* conditions is not known. Therefore, to validate the use of intra-IO carbenoxolone injection under the present experimental conditions, we first measured the effect of the injections on the climbing fiber reflex. The climbing fiber reflex refers to the phenomenon that electrical stimulation of the cerebellar white matter causes an antidromic activation of the olivocerebellar axons, and then a return orthodromic spike volley that produces CSs. The antidromic invasion of an IO neuron causes current to flow from it, via gap junctions, to its neighbors, leading to orthodromic responses (Llinás et al., 1974), which is why the reflex can be used as a measure of electrical coupling between IO neurons.

Climbing fiber reflex responses were evoked before (control) and after injection of carbenoxolone into the IO in three experiments in which recording arrays were placed on crus 2a ($n = 94$ cells). Responses were evoked by brief (100 μ s) current pulses applied via a bipolar metal electrode inserted into the cerebellar white matter. In cells showing responses, stimuli typically produced both an initial short-latency response (Fig. 2A1, arrowhead), attributable to axonal branching of olivocerebellar axons, and a second longer-latency, climbing fiber reflex response (Fig. 2A1, arrow). Although for a particular cell both responses were often evoked, the two responses were not absolutely correlated, so that after some stimuli the cell might show only one of the two responses.

Approximately 300 stimuli were given in each condition, and the response distribution determined from peristimulus histograms, such as those shown in Figure 2B, which plot response probability as a percentage of the total number of stimuli. In each experiment, the evoked responses occurred in a subset of cells that formed a cluster spanning two to four rostrocaudally oriented columns (Fig. 2C1). Thus, in control, 25 cells in the three experiments showed responses and typically had a bimodal response pattern, with peaks occurring at 3.88 ± 0.34 and 8.94 ± 0.72 ms latencies, corresponding to the short-latency and reflex responses. Note that the latency of the second peak corresponds to approximately twice the ~ 4 ms conduction time of the olivocerebellar pathway in rats (Sugihara et al., 1993), consistent with its route through the IO. Also note that the response distribution of the reflex is consistent with the topography of the olivocerebellar pathway, in which neighboring IO neurons tend to project to rostrocaudally oriented cortical strips.

Injection of carbenoxolone into the IO produced a large reduction or disappearance of the climbing fiber reflex response in cells without affecting the short-latency response probability. The effect of carbenoxolone is shown for one cell in Figure 2, A and B, and for one experiment in Figure 2C, in which the circles' positions reflect the relative locations of the cells in the recording array and their areas are proportional to the response percentage. Averaged across all 25 cells that showed responses in control, carbenoxolone produced a 69% drop in the reflex response probability (control, $12.1 \pm 1.49\%$; carbenoxolone, $3.8 \pm 0.53\%$; $p = 2.16 \times 10^{-7}$). In contrast, there was no significant change in the short-latency response rate (control, $50.6 \pm 5.1\%$; carbenoxolone, $58.3 \pm 7.0\%$; $p = 0.14$), indicating that

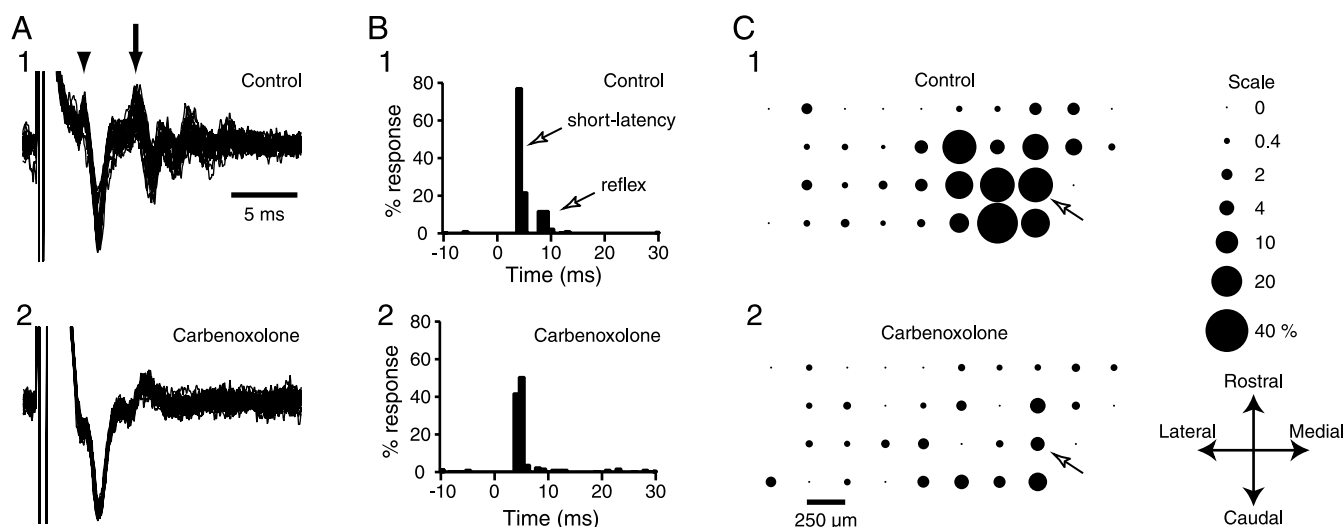


Figure 2. Intra-IO injection of carbenoxolone blocks the climbing fiber reflex. **A**, Responses evoked by cerebellar white matter stimulation before (**A1**) and after (**A2**) carbenoxolone administration. **A1**, Ten overlapped traces showing responses in control condition that have both short-latency (arrowhead) and reflex (arrow) components. Initial deflection is stimulus artifact. **A2**, Responses to an identical strength stimulus during intra-IO injection of carbenoxolone. Short-latency response is present, but reflex response is no longer elicited. **B**, Peristimulus histogram of cell in **A** showing the short-latency (~ 4 ms) and reflex responses (~ 8 – 12 ms) in control (**B1**) and during carbenoxolone (**B2**) to ~ 300 stimuli. Bin size, 1 ms. **C**, Bubble representation of climbing fiber reflex response in control (**C1**) and during carbenoxolone (**C2**) across the entire recording array. The bubble size reflects the percentage of responses to ~ 300 stimuli according to the scale on the right. The key at the bottom right indicates the orientation of the array on crus 2a. The arrow indicates the location of the cell whose histograms are shown in **B**.

the axonal activation produced by the stimulus remained consistent across experimental conditions.

Spontaneous CS experiments

The above results suggest that intra-IO injections of carbenoxolone cause a substantial reduction in electrotonic coupling between IO neurons. Therefore, the effect of these injections on spontaneous CS activity was investigated. A total of 165 crus 2a Purkinje cells in nine experiments (12–30 cells per experiment) were recorded for this purpose. In each experiment, a 20 min control recording was followed by injection of carbenoxolone into the IO. Based on time course experiments (see below), which showed that the effects of the injection become stable after ~ 40 min, the injection was continued for ~ 60 min, and the last 10–20 min were used for the analyses below. Comparison of the control and drug injection conditions revealed major effects on CS activity including a decrease in average firing rate, a decrease in synchrony, and a decrease in rhythmicity. These effects are described in turn below.

Carbenoxolone decreases average CS firing rate

In control, the average CS firing rate, computed from 165 cells in nine experiments, was 1.38 ± 0.70 Hz. Injection of carbenoxolone resulted in a significantly lower firing rate of 0.69 ± 0.58 ($p \sim 0$), which represented a 50% decrease from the control rate. This effect was consistently observed: carbenoxolone caused a statistically significant drop in the average firing rate in all experiments ($p \leq 0.007$). Moreover, the vast majority (92%) of cells decreased their firing rate with carbenoxolone.

Carbenoxolone decreases both intraband and interband synchrony

A similarly consistent effect on CS synchrony was also observed. In all nine experiments, carbenoxolone injection caused a significant drop in average synchrony ($p \leq 0.046$). Averaged across all cell pairs, carbenoxolone decreased CS synchrony by 50% from control levels (control, 0.0250 ± 0.0366 ; carbenoxolone, 0.0125 ± 0.0250 ; $n = 1523$ cell pairs; $p \sim 0$, paired t test), with

$\sim 93\%$ of cells showing a decrease. Note that a decrease in synchrony does not automatically result from the decreased firing rates described above because the cross-correlation formula used for the calculation is normalized for firing rate. Moreover, even with the lower firing rates, each cell fired over 800 spikes on average during the recording session, so that the datasets for the calculation were still quite large.

In control conditions, the distribution of CS synchrony among the cell pairs is not random but rather varies with the distance separating two cells (Sasaki et al., 1989; Sugihara et al., 1993; Lang et al., 1999). Specifically, synchrony levels tend to remain high with increasing separation in the rostrocaudal direction (transverse axis of the folium) but fall rapidly as the distance between two cells increases in the mediolateral direction (longitudinal folial axis). Thus, cells with synchronous CSs tend to be located within a rostrocaudally oriented cortical strip that is typically 250 – $500 \mu\text{m}$ wide. This banding pattern can be demonstrated by plotting the average synchrony for cell pairs as a function of the separation distance in the mediolateral direction (longitudinal axis of the folium) of the cells in a pair. Such a plot (Fig. 3A, filled circles), using all cell pairs from all nine experiments, shows that CS synchrony is high for cells having small mediolateral separations (0 – $250 \mu\text{m}$, intraband pairs) and then falls to low levels for more widely separated cells (interband pairs), consistent with previous findings (Sasaki et al., 1989; Sugihara et al., 1993; Lang et al., 1999).

It is possible that synchronous activity in these two classes of cell pairs (interband and intraband) is generated by distinct mechanisms. Indeed, this possibility was raised by previous work showing that interband and intraband synchrony are differentially affected by block of IO afferents (Lang, 2001). However, comparison of the two curves in Figure 3A shows carbenoxolone produced a significant drop in synchrony for all separation distances except the largest ones (1750 – $2250 \mu\text{m}$), suggesting that gap junction coupling underlies both intraband and extraband synchrony.

Nevertheless, the strength of the effect of carbenoxolone on synchrony showed a complex variation with separation distance

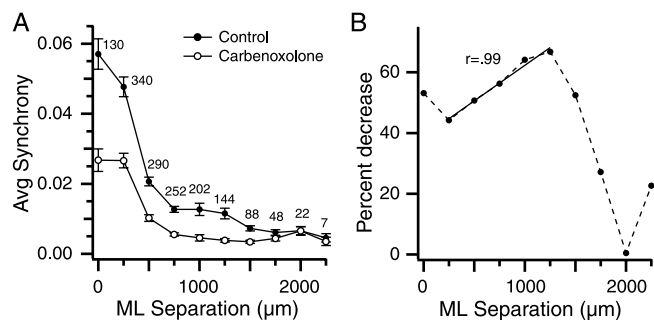


Figure 3. Intra-IO carbenoxolone reduces CS synchrony levels. **A**, Average CS synchrony calculated from all cell pairs in all experiments and plotted as a function of the mediolateral (ML) distance between the cells in a pair. The number above each data point indicates the number of cell pairs at that separation. Error bars are SE. **B**, Percent decrease in synchrony from control levels caused by carbenoxolone injection plotted as a function of mediolateral separation between cells. Solid line, Least-squares regression line to points at 250–1250 μm separations. Pearson's r ($=0.98$) indicates correlation coefficient for the x and y variables for the data in the same range.

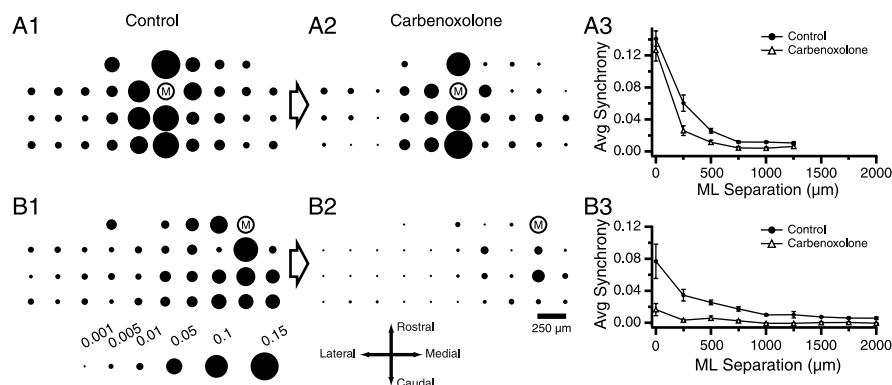


Figure 4. Intraexperiment variation in the effect of carbenoxolone on synchrony. **A**, **B**, Synchrony distribution with respect to two reference cells labeled "M" from the same experiment. Bubble plot representations of the synchrony distributions are shown for each cell in control (**A1**, **B1**) and during injection of carbenoxolone into the IO (**A2**, **B2**). The cell in **A** shows only a modest decrease in synchrony, whereas that in **B** shows a near-complete desynchronization. **A3**, **B3**, Plots of average CS synchrony as a function of mediolateral separation between cells. Average synchrony is plotted for all cell pairs that include the reference cell shown in the corresponding bubble plots. Note that the curves in **A3** end at 1250 μm because the reference cell is located in the middle of the array, and this value corresponds to the distance from the reference cell to the farthest (lateral) border of the array. Error bars are SE. ML, Mediolateral.

between cells (Fig. 3B, dotted line). For separations between 250 and 1250 μm , the percent drop increased in a linear manner (solid line, $r = 0.99$), probably reflecting the increased tenuousness of the coupling between IO cells projecting to different cerebellar zones; however, the percent drop decreased rapidly for still greater separations. This reduction is most likely attributable to a floor effect, because the control synchrony levels at these distances were already close to chance levels (Sugihara et al., 1993). The results of experiments with picrotoxin presented below support this view (see Fig. 9).

Intercell variation of the effect of carbenoxolone on CS synchrony

Although carbenoxolone produced a 50% overall reduction in synchrony, this result could be interpreted to suggest that there are significant non-gap junction-related mechanisms underlying the remaining synchrony. This issue is taken up further in Discussion, but here results concerning the variation of the effect of carbenoxolone from cell to cell within individual experiments are described to address this issue.

Despite the fact that carbenoxolone reduced both intraband

and interband synchrony, its effectiveness could vary considerably among cells within a given experiment. Bubble plots (Fig. 4A1,A2,B1,B2) and synchrony versus mediolateral separation curves (Fig. 4A3,B3) for two cells from the same experiment provide an example of this variability. In control (Fig. 4A1,B1), both cells showed synchrony distributions in which synchronous CSs occurred most often with their respective neighbors to form rostrocaudally oriented cell bands, as shown in the bubble plots by the large circles that neighbor each reference cell, and in the synchrony curves by their decrease in average synchrony with distance. The effect of carbenoxolone injection on the synchronous CS activity of these two cells can be seen to be quite different. For the cell of Figure 4A, only a modest decrease in CS synchrony occurred, whereas for the cell of Figure 4B carbenoxolone injection resulted in a near complete loss of synchrony. Such response variability was observed in most experiments, with the difference between the maximum and minimum percent decrease value for individual cells in an experiment averaging $67.8 \pm 22.1\%$ ($n = 9$).

There are several possible explanations for this variability; however, the most likely one relates to the fact that the recording array spans ~ 2.25 mm along the longitudinal axis of crus 2a, and that the climbing fibers projecting to this expanse arise from distinct regions of the IO. Thus, there may have been variable delivery of carbenoxolone to these IO areas, resulting in different levels of blockade of gap junctions.

To test this possibility, we made use of the fact that each region of the rat IO projects to a narrow rostrocaudally oriented strip of cortex (Buisseret-Delmas and Angaut, 1993; Sugihara and Shinoda, 2004), which corresponds to approximately two to three columns of cells in the recording array. Because we did not know the actual borders of the projection zones, we used a sliding window of three columns (Fig. 5A, gray rectangle) and calculated the change in CS synchrony caused by carbenoxolone for the cells in each three-column

group. This analysis was performed on eight experiments, the results from four of them are shown in Figure 5B, and demonstrate the range of what was observed. In these plots, zero on the abscissa corresponds to the lateralmost three-column group, and each increment of one corresponds to a 250 μm shift of the cell column group (i.e., a shift of one column in the recording array).

Examination of these plots shows that, in some experiments (Fig. 5B, experiment 1), a high, relatively uniform block of synchrony was achieved, suggesting that carbenoxolone was delivered throughout much of the IO. However, in most cases, the effect was more variable (Fig. 5B, experiments 2–4). In all experiments, there was at least one region showing a large percent decrease in synchrony. Indeed, in all eight experiments, at least one cell column group had a $>50\%$ decrease; in four experiments, at least one group showed a $>70\%$ decrease; and two experiments had groups with $>80\%$ decreases. Lastly, it is worth noting that the location of the cell group showing the maximal percent decrease in synchrony varied between experiments. Because the grid placement in the various experiments was relatively constant, this result suggests that carbenoxolone can similarly affect gap junction coupling in different IO regions.

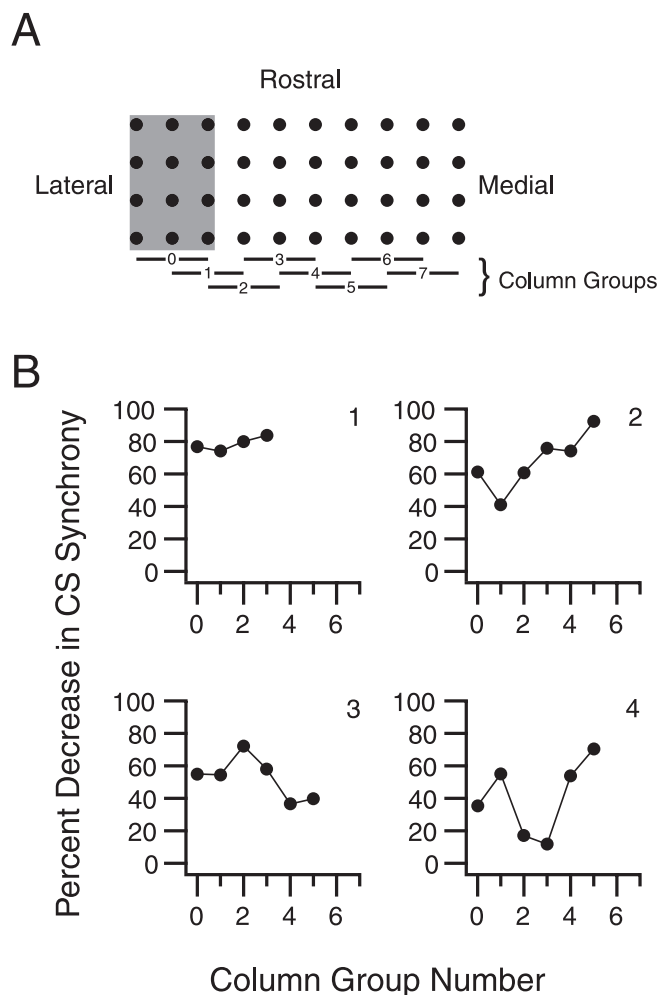


Figure 5. Inter-column variation of the effect of carbenoxolone on synchrony. **A**, Black dots represent electrode positions in a 4×10 recording array, which is shown to illustrate the analysis procedure. Electrodes were grouped into sets of three adjacent rostrocaudally running columns. Average synchrony was then calculated for each cell group using all of its cell pairs. Horizontal bars show column groupings that were used. The bar numbers correspond to the abscissa values in the plots in **B**. The lateralmost group, group 0, is indicated by the gray rectangle. **B**, Plots of percent decrease in CS synchrony with carbenoxolone as a function of rostrocaudal column location on recording array. Each plot shows the results from a single experiment.

Dose–response and time course curves for the effect of carbenoxolone on CS activity

Carbenoxolone has been shown to block IO gap junctions at concentrations of $\sim 200 \mu\text{M}$ *in vitro* (Leznik, 2004). However, a somewhat higher concentration ($500 \mu\text{M}$) was used in the present experiments because carbenoxolone was delivered into the IO from a point source from which a concentration gradient would exist. Indeed, the above results (Fig. 5) suggest that diffusion limitations may have prevented the observance of a greater overall effect of carbenoxolone on CS activity. To test whether significantly greater effects could be obtained with higher carbenoxolone concentrations, dose–response curves were obtained in three animals ($n = 62$ cells), and the average firing rate and CS synchrony were calculated for each concentration. At each concentration level, carbenoxolone was injected for 60 min and the last 20 min were analyzed. In all experiments, both CS firing rate (Fig. 6A, filled circles) and synchrony (Fig. 6A, open circles) decreased sharply as the concentration of carbenoxolone was increased up to $500 \mu\text{M}$, whereas additional increases in concentration produced much smaller changes in CS activity.

A second factor related to whether carbenoxolone achieved its maximal block is the injection duration. As stated above, analyses for the carbenoxolone conditions were performed on recordings made ~ 40 min after the drug injection into the IO had begun. This delay was chosen on the basis of three experiments ($n = 61$ cells) like the one shown in Figure 6B, in which the average firing rate (filled circles) and CS synchrony (open circles) levels can be seen to decrease in parallel from control levels over the course of 20–30 min before stabilizing. In the other experiments, firing rate stabilized at 30 min in both cases, and synchrony stabilized at 30 and 45 min.

Carbenoxolone injection decreases CS rhythmicity

To investigate whether gap junction coupling influences CS rhythmicity, autocorrelograms were made of the activity of each cell in control and carbenoxolone conditions. Comparison of these correlograms suggested that CS rhythmicity was reduced by carbenoxolone. However, because of the low firing rates in the carbenoxolone condition, it was hard to quantify this change using the individual cell correlograms. Thus, population histograms were generated by summing the individual cell correlograms for each experiment. In seven of eight experiments, the carbenoxolone condition autocorrelograms had a significantly ($p < 0.02$) lower amplitude primary peak.

To investigate whether the loss of rhythmicity was correlated with a loss of synchrony, cells from all experiments were combined and grouped according to their percent decrease in synchrony: 0–20, 20–40, 40–60, 60–80, and 80–100%. All experiments had cells that fell into at least two groups, and most experiments (six of eight) had cells distributed to four or five groups. Population autocorrelograms were then generated for each group for control and carbenoxolone conditions (Fig. 7A). Cells with small decreases in synchrony ($< 20\%$) showed no change in the height of the primary peak, whereas for cells with the largest synchrony decreases (80–100%) the primary peak in the autocorrelogram was abolished, and cells showing intermediate level of synchrony decrease, had a partial reduction in the size of their autocorrelogram primary peaks. The reduction in peak amplitude was significant ($p < 0.006$) for all groups except the 0–20% group. Figure 7B plots the change in primary peak area as a function of the decrease in synchrony for the groups. Again, a strong correlation was found between the two variables.

Picrotoxin and NBQX-induced changes in CS synchrony are antagonized by carbenoxolone injection

Previous studies showed that block of GABAergic activity in the IO by local picrotoxin injection increased CS synchrony, whereas block of glutamatergic activity with NBQX injections led to more restricted synchrony distributions (Lang et al., 1996; Lang, 2001, 2002). These changes in synchrony distribution were attributed to the modification of the effective coupling of IO neurons via gap junctions by these transmitters. If this is correct, carbenoxolone injections should limit or reverse the changes in synchrony distribution caused by these receptor antagonists.

Thus, in five experiments ($n = 121$ cells), picrotoxin was injected into the IO. This injection produced effects similar to those previously reported. Average firing rate increased 49% (control, 1.37 ± 0.77 ; picrotoxin, 2.04 ± 1.06 ; $p = 2.16 \times 10^{-12}$), and synchrony increased 196% (control, 0.0234 ± 0.0350 ; picrotoxin, 0.0693 ± 0.0686 ; $n = 1465$ cell pairs; $p \sim 0$). Addition of carbenoxolone to the injection solution resulted in significant decreases in average firing rate (46%; 1.10 ± 0.78 ; $p \sim 0$) and synchrony (37%; 0.0438 ± 0.0567 ; $p \sim 0$) from the picrotoxin

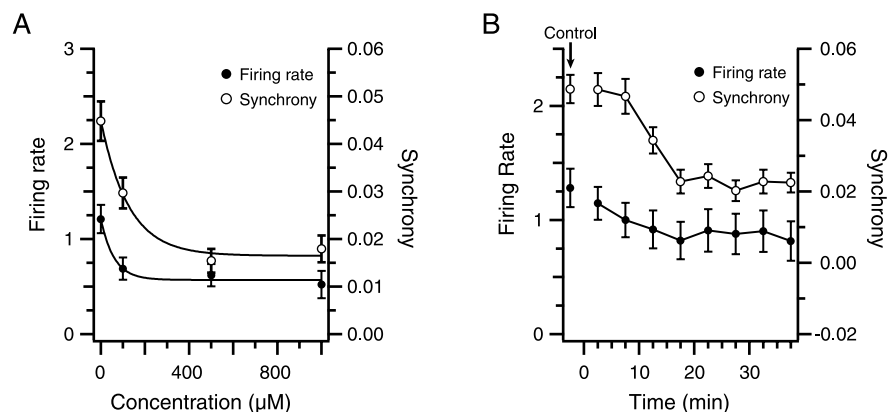


Figure 6. Dose–response and time course curves for the effect of carbenoxolone on CS activity. **A**, Dose–response curves were obtained by plotting average firing rate (left axis, filled circles) and synchrony (right axis, open circles) as a function of carbenoxolone concentration. Zero concentration points represent control values before start of injection. At each concentration, carbenoxolone was injected for 40 min before recording CS activity for 20 min. Injection solutions were switched with the pipette remaining in place in the IO. In this experiment, 24 cells were simultaneously recorded. Curves are least-squares fits to the data. **B**, Time course of the effect of carbenoxolone. The plot shows average firing rate and synchrony as a function of time after start of injection for an experiment in which 19 cells were recorded simultaneously. Each data point represents a 5 min recording period centered about the x-coordinate of the point, except for the control points (arrow), which were obtained from a 20 min recording before the start of the injection. Error bars in **A** and **B** are SE.

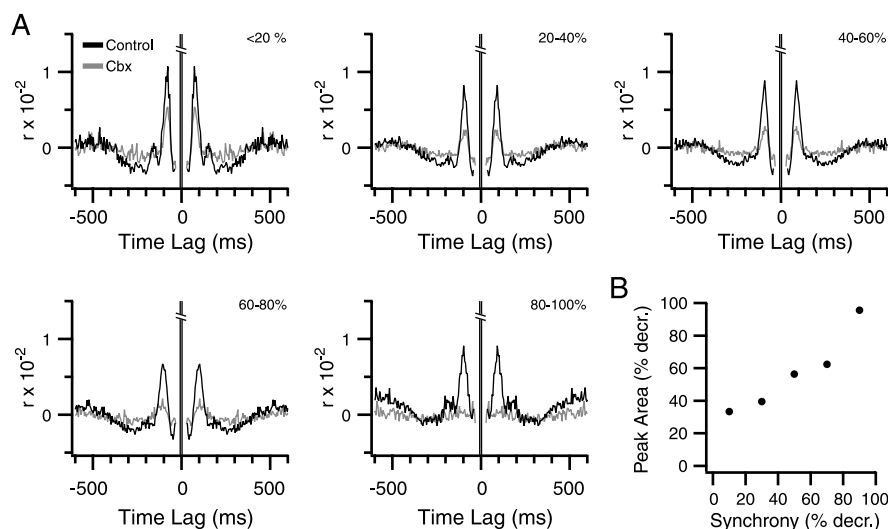


Figure 7. Carbenoxolone injection reduces CS rhythmicity: comparison across cell groups. **A**, Cells from all experiments were grouped according to their percent decrease in synchrony. Population autocorrelograms are shown for each of the groups, with the group ranges indicated in top right of each correlogram. The control correlograms are shown in black; the carbenoxolone (CbX) correlograms are in gray. **B**, Plot of percent decrease in synchrony versus percent decrease in primary autocorrelogram peak area between control and carbenoxolone for the same synchrony groups as in **A**. Midpoints of synchrony ranges were used for abscissa values.

condition. An example of the increase in synchrony caused by picrotoxin and its subsequent decrease with carbenoxolone is shown in Figure 8.

The bubble plots show the change in synchrony distribution by successive drug injections into the IO (Fig. 8A). Picrotoxin produced a widespread synchrony distribution (Fig. 8A2, Ptx); however, when carbenoxolone was added to the solution and both drugs were co-injected, a dramatic decrease in synchrony resulted (Fig. 8A3, Ptx + Ctx). The effect on synchrony of the two injections (picrotoxin and picrotoxin plus carbenoxolone) are further compared in Figure 8, B1 and B2, respectively, which show the changes in CS synchrony caused by addition of each drug. In each case, the initial condition is shown by the filled circles and the latter one by open circles. These two plots were

generated using all cell pairs ($n = 465$ pairs; 31 cells) in this experiment and show the large increase in synchrony caused by picrotoxin and its subsequent reversal by carbenoxolone. A similar plot using all cell pairs from all experiments indicates that the action of carbenoxolone to reduce high, picrotoxin-induced synchrony levels was consistently found (Fig. 9A). Moreover, carbenoxolone also produced a large (58.3%) percent drop in climbing fiber reflex responses (response rate: picrotoxin, $33.7 \pm 3.9\%$; picrotoxin plus carbenoxolone, $14.4 \pm 2.5\%$; $p = 7.0 \times 10^{-9}$; $n = 36$ cells; $n = 2$ experiments).

The widespread synchrony distribution after picrotoxin also allowed an additional examination of the question of whether carbenoxolone blocks CS synchrony between cells that are widely separated along the longitudinal axis of the folium. From Figures 8 and 9A, it is clear that carbenoxolone reduced synchrony in the presence of picrotoxin regardless of the distance separating cells along the longitudinal axis of the folium. Furthermore, the relative drop in synchrony increased linearly with separation (Fig. 9B), in contrast to what was observed for the carbenoxolone-only experiments, in which the relative effect of carbenoxolone decreased for the largest separations (Fig. 3). This result suggests that the decrease seen in Figure 3 at large separation distances reflected a floor effect.

To investigate whether excitatory afferent input underlay the synchrony that remained after combined injection of picrotoxin and carbenoxolone, the glutamate antagonist NBQX was subsequently added to the injection solution ($n = 100$ cells; four experiments). Addition of NBQX produced a small (21%) additional decrease in firing rate (picrotoxin plus carbenoxolone, 1.15 ± 0.81 ; picrotoxin plus carbenoxolone plus NBQX, 0.91 ± 0.75 ; $p = 0.0006$), but no change in synchrony (picrotoxin plus carbenoxolone, 0.0467 ± 0.0576 ; picrotoxin plus carbenoxolone plus NBQX, 0.0465 ± 0.0564 ; $n = 1255$

cell pairs; $p = 0.77$). The lack of effect on synchrony with addition of NBQX is illustrated for one experiment in Figure 8. The bubble plots in Figure 8, A3 and A4, are quite similar, as are the synchrony curves shown in Figure 8B3. In addition to the above four experiments, NBQX was added to the injection solution after first injecting carbenoxolone alone in one case, and produced no additional change in CS synchrony (data not shown).

Because NBQX had little effect on the spontaneous activity when injected after carbenoxolone, its efficacy in blocking excitatory afferents to the IO was verified by monitoring CS responses evoked by electrical stimulation of the vibrissal region of the motor cortex ($n = 101$ cells, 3 experiments). During picrotoxin injection into the IO, stimuli evoked CSs at latencies of 15–22 ms in most of the cells in the array, such that there was an overall rate of

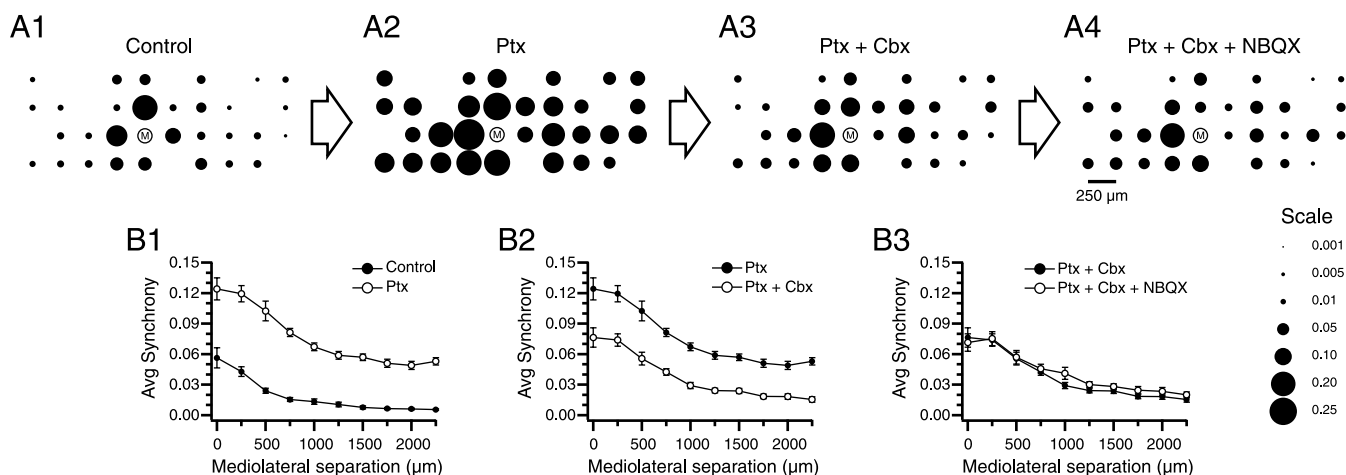


Figure 8. Picrotoxin- and NBQX-induced changes in synchrony are antagonized by carbenoxolone. **A**, Bubble plots showing CS synchrony with respect to a reference cell (labeled "M") in a sequence of experimental conditions in which drugs were injected into the IO. From left to right, the drug combinations listed above the bubble plot were injected into the IO. Ptx, Picrotoxin; Cbx, carbenoxolone. The synchrony scale is in the bottom right corner. **B**, Plots of average synchrony as a function of mediolateral separation between cells. All cell pairs from the array shown in the top row (not just those pairs containing cell M) were used to generate the plots. Each plot shows the synchrony curves for two successive conditions: **B1** shows traces corresponding to **A1** and **A2** conditions; **B2** shows traces for **A2** and **A3** conditions; and **B3** shows traces for **A3** and **A4** conditions. Error bars are SE.

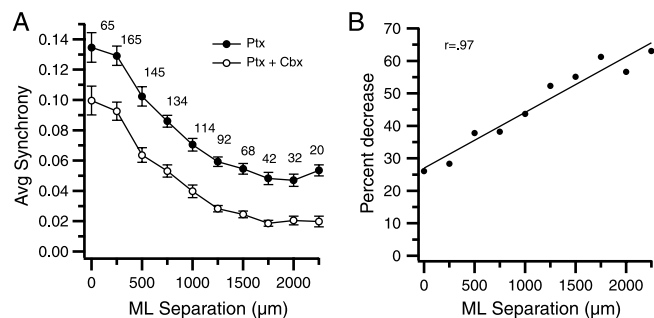


Figure 9. Intra-IO carbenoxolone lowers picrotoxin-enhanced synchrony. **A**, Average CS synchrony calculated from all cell pairs in all experiments and plotted as a function of the mediolateral distance between the cells in a pair for picrotoxin (Ptx) and picrotoxin plus carbenoxolone (Ptx + Carb) conditions. The number above each data point indicates the number of cell pairs at that separation. Error bars are SE. **B**, Percent decrease in synchrony from picrotoxin-alone condition caused by addition of carbenoxolone to the injection solution plotted as a function of mediolateral separation between cells. The solid line is least-squares regression line. ML, Mediolateral.

$33.46 \pm 3.42\%$. Addition of carbenoxolone produced a modest (27.8%) but statistically significant decrease in overall response rate (picrotoxin plus carbenoxolone, $24.13 \pm 1.9\%$; $p \sim 0$), suggesting that electrotonic coupling contributes to the responsiveness of the cells to the stimuli. The further addition of NBQX to the IO injection solution caused a virtual elimination of motor cortex-evoked responses ($3.37 \pm 0.62\%$; $p \sim 0$), demonstrating that NBQX was indeed blocking glutamatergic IO afferents.

Discussion

The major conclusions of this paper are that (1) CS synchrony is dependent on gap junction coupling of IO neurons, (2) tonic GABA and glutamate release in the IO change CS synchrony patterns via a mechanism involving IO gap junctions, (3) electrotonic coupling between IO neurons contributes to spontaneous CS activity levels, and (4) CS rhythmicity depends on electrotonic coupling of IO neurons.

Gap junction coupling between IO neurons mediates CS synchrony

Synchronous CS activity was first reported by Bell and Kawasaki (1972). Subsequently, gap junctions were found to couple IO

neurons electrotonically, leading to the hypothesis that synchronous CS activity was attributable to this coupling (Llinás et al., 1974; Sotelo et al., 1974). Since then, the patterns of synchronous CS activity have been characterized in detail (Llinás and Sasaki, 1989; Sasaki et al., 1989; Sugihara et al., 1993; Lang et al., 1999). Yet, beyond directly demonstrating that IO neurons are coupled (Llinás and Yarom, 1981a), the central tenet of this hypothesis, namely that CS synchrony is the result of gap junction coupling of IO neurons, was not directly tested until the present study.

Several lines of evidence are consistent with this hypothesis: the density of dendritic lamellar bodies, an organelle associated with gap junctions (De Zeeuw et al., 1995), in different floccular projecting regions of the IO correlates with the CS synchrony level in their corresponding target areas (De Zeeuw et al., 1997); CS synchrony remains after block of glutamatergic and/or GABAergic IO afferents, which provide the main synaptic input to the IO, providing support for the gap junction hypothesis by process of elimination (Lang et al., 1996; Lang, 2001, 2002); *in vitro* studies of IO neurons in connexin36 knock-out mice showed that IO subthreshold oscillations in neighboring cells, which are in phase in normal animals, are not so in the knock-out (Long et al., 2002); CS synchrony is greatly reduced in the connexin36 knock-outs compared with normal mice (Marshall et al., 2004); application of gap junction blockers to IO slices leads to desynchronization of the IO subthreshold oscillations (Leznik and Llinás, 2005).

Although these studies provide support for the hypothesis that gap junctions synchronize CS activity, concerns can be raised against each because of their correlative or indirect natures. For example, in the case of the synaptic block experiments, there are other synaptic inputs to the IO that were not tested; with regard to the knock-out mice, developmental compensations are always an issue. Moreover, the *in vitro* studies investigated subthreshold oscillations (or spike activity related to them), which have yet to be shown under *in vivo* conditions, and whose characteristics (e.g., frequency, stability) raise questions about their relationship to CS activity.

Thus, the present results are significant, because they provide the first direct evidence that gap junction coupling of IO neurons underlies CS synchrony, because acute block of gap junctions in the IO by carbenoxolone led to large reductions in synchrony.

Moreover, given that projections to the recording area arise from all three major subdivisions of the IO (I. Sugihara, S. P. Marshall, E. J. Lang, unpublished observations), our results suggest that gap junction coupling is the general mechanism for synchronizing IO spike activity.

Before accepting the above conclusion, it is important to consider why the carbenoxolone injections only reduced synchrony instead of abolishing it, and whether this implies the existence of additional mechanisms by which CS synchrony is generated. Indeed, *a priori*, it seems reasonable that simultaneous activity in IO afferents could lead to synchronous CSs. In fact, increased CS synchrony occurs during motor cortex stimulation (Lang, 2002). Yet, given normal, tonic levels of IO afferent activity, our results suggest that gap junction coupling underlies the vast majority of CS synchrony. In particular, synchrony levels during carbenoxolone injection were unchanged by the addition of NBQX, suggesting that simultaneous spikes embedded within IO afferent activity do not trigger significant numbers of synchronous events. Moreover, near-complete (>80%) loss of synchrony was sometimes achieved for local clusters of cells (Fig. 5).

The persisting synchrony during carbenoxolone administration most likely reflected technical limitations. Specifically, the regional variation in synchrony loss (Fig. 5), combined with the fact that climbing fiber projections to crus 2a arise from multiple IO regions (Buisseret-Delmas and Angaut, 1993; Sugihara and Shinoda, 2004), suggest that diffusion barriers were a major reason for the incomplete loss of synchrony. Another factor is that carbenoxolone does not completely block electrical coupling (Rozental et al., 2001), as confirmed by the climbing fiber reflex results.

It is also important to consider whether the effect of carbenoxolone on CS synchrony could be attributable to loss of coupling among glial cells in the IO, particularly because Ca waves in astrocytes can synchronize neuronal activity via glutamate release and the resulting activation of NMDA receptors (Reinhardt Parri et al., 2001; Fellin et al., 2004). However, the rarity (<1 min⁻¹) and lack of temporal precision (~100 ms timescale versus ~1 ms for CS synchrony) of glial-mediated synchronizing events makes this an unlikely explanation. Moreover, our experiments were performed under ketamine, an NMDA receptor antagonist, and yet CS synchrony was present in control.

In sum, the results indicate electrotonic coupling of IO neurons is the predominant mechanism underlying CS synchrony. And thus it follows that, in the absence of a strong stimulus, olivary afferents only play a modulatory role in sculpting out the cell clusters whose activity is synchronized, but do not directly provide the synchronizing signal themselves, which is consistent with previous work (Lang 2001, 2002).

Gap junction coupling helps determine IO excitability

The present results suggest that electrical coupling plays a role in determining the excitability of IO neurons, and hence the average levels of CS activity. Indeed, the ~50% drop in CS firing rate with only a partial block of coupling suggests a major role. These results are consistent with those showing that waves of synchronous CSs travel across the cerebellar cortex (Yamamoto et al., 2001) and suggest that the synchronous activity in one cluster of IO neurons triggers activity in neighboring cell clusters.

It is possible that the decreased firing rates may have been attributable to non-gap junction-related effects of carbenoxolone, because it can affect other membrane conductances (Rozental et al., 2001), and has been reported to change the resting potential of endothelial and smooth muscle cells (Tare et al., 2002). However, carbenoxolone does not change the resting po-

tential of IO neurons, nor does it affect the major voltage-gated conductances that contribute to IO excitability (Placantonakis et al., 2004; Leznik and Llinás, 2005). It does have some minor effects on the passive membrane properties of IO neurons (at least partly because of its block of coupling), including increasing the input resistance slightly (Placantonakis et al., 2004; Leznik and Llinás, 2005), but this would not be expected to decrease the firing rate. Also, a glial-mediated effect is unlikely, because a loss of spatial K buffering capability attributable to decoupling of glial cells, would, if anything, tend to depolarize the cells, making them more excitable.

Dependence of CS rhythmicity on gap junction coupling of IO neurons

IO neurons have membrane conductances that could lead to rhythmic spiking via the interaction of a high threshold Ca spike that triggers a prolonged afterhyperpolarization, which in turn leads to a low-threshold rebound Ca spike (Llinás and Yarom, 1981a,b; Bal and McCormick, 1997). However, IO neurons also display subthreshold oscillations *in vitro*, which may underlie rhythmic CS activity. Although these oscillations are dependent on the above-mentioned conductances, they are a population phenomenon, and thus it has been suggested that they also require electrical coupling between IO neurons (Llinás and Yarom, 1986; Yarom, 1991; Lampl and Yarom, 1997). Indeed, although the major membrane conductances of IO neurons are present during the first postnatal week, subthreshold oscillations do not appear until postnatal days 10–15 when gap junctions become functional (Bleasel and Pettigrew, 1992). Modeling results have also suggested a linkage between electrotonic coupling and spontaneous oscillations by showing that simulated IO neurons, which do not show spontaneous oscillations in isolation, do so when coupled to each other (Manor et al., 1997).

However, the necessity of electrotonic coupling for generating these subthreshold oscillations has been questioned. For example, subthreshold oscillations were found to remain following application of gap junction blockers to IO slices (Leznik and Llinás, 2005). Moreover, the oscillations were found in connexin36 knock-out mice, in which coupling between IO neurons is greatly reduced (Long et al., 2002). However, a subsequent study found compensatory changes in IO neurons in these mice that might explain their ability to oscillate in the absence of coupling (De Zeeuw et al., 2003).

Thus, controversy exists over whether gap junction coupling is necessary for generating olivary rhythmicity. Our results suggest that they do in fact play an important role. In particular, we found that carbenoxolone injections reduced CS rhythmicity, and that the extent of this reduction varied with the level of synchrony loss. Although in some experiments there was a complete loss of the autocorrelogram peaks reflecting the ~10 Hz rhythmicity, in most cases only a reduction was observed. This incomplete loss most likely reflects the partial block of gap junctions that was achieved by the injections, a point reinforced by the correlation shown in Figure 7B. However, it is also possible that some individual olivary neurons are spontaneous oscillators, which is consistent with the fact that some cells continued to display rhythmic CS activity despite large drops in synchrony. In comparing our results with those of *in vitro* studies, it is also important to remember that subthreshold oscillations and rhythmic CS activity are distinct phenomena whose relationship remains to be determined, although almost certainly both arise from the same set of membrane conductances. Nevertheless, our results suggest a close tie between the electrical coupling of IO

neurons and their oscillatory behavior. This conclusion is consistent with previous results demonstrating a covariance between levels of CS rhythmicity and synchrony in normal animals, and with the fact that manipulations that alter the pattern of coupling can change the stability and frequency characteristics of oscillatory CS activity (Lang et al., 1996; Lang, 2001).

References

- Bal T, McCormick DA (1997) Synchronized oscillations in the inferior olive are controlled by the hyperpolarization-activated cation current I_h . *J Neurophysiol* 77:3145–3156.
- Bell CC, Kawasaki T (1972) Relations among climbing fiber responses of nearby Purkinje cells. *J Neurophysiol* 35:155–169.
- Belluardo N, Mudò G, Travato-Salinario A, Le Gurun S, Charollais A, Serre-Bienier V, Amato G, Haefliger J-A, Meda P, Condorelli DF (2000) Expression of connexin36 in the adult and developing rat brain. *Brain Res* 865:121–138.
- Benardo LS, Foster RE (1986) Oscillatory behavior in inferior olive neurons: mechanisms, modulation, cell aggregates. *Brain Res Bull* 17:773–784.
- Bleasell AF, Pettigrew AG (1992) Development and properties of spontaneous oscillations of the membrane potential in inferior olivary neurons in the rat. *Brain Res Dev Brain Res* 65:43–50.
- Buisseret-Delmas C, Angaut P (1993) The cerebellar olivo-corticonuclear connections in the rat. *Prog Neurobiol* 40:63–87.
- Condorelli DF, Parenti R, Spinella F, Salinaro AT, Belluardo N, Cardile V, Cicirata F (1998) Cloning of a new gap junction gene (Cx36) highly expressed in mammalian brain neurons. *Eur J Neurosci* 10:1202–1208.
- Crill WE (1970) Unitary multiple-spiked responses in cat inferior olive nucleus. *J Neurophysiol* 33:199–209.
- Crill WE, Kennedy TT (1967) Inferior olive of the cat: intracellular recording. *Science* 157:716–718.
- Devor A, Yarom Y (2002) Electrotonic coupling in the inferior olivary nucleus revealed by simultaneous double patch recordings. *J Neurophysiol* 87:3048–3058.
- De Zeeuw CI, Holstege JC, Ruigrok TJH, Voogd J (1989) Ultrastructural study of the GABAergic, cerebellar, and mesodiencephalic innervation of the cat medial accessory olive: anterograde tracing combined with immunocytochemistry. *J Comp Neurol* 284:12–35.
- De Zeeuw CI, Hertzberg EL, Mugnaini E (1995) The dendritic lamellar body: a new neuronal organelle putatively associated with dendrodendritic gap junctions. *J Neurosci* 15:1587–1604.
- De Zeeuw CI, Koekkoek SKE, Wylie DRW, Simpson JI (1997) Association between dendritic lamellar bodies and complex spike synchrony in the olivocerebellar system. *J Neurophysiol* 77:1747–1758.
- De Zeeuw CI, Chorev E, Devor A, Manor Y, Van Der Giessen RS, De Jeu MT, Hoogenraad CC, Bijman J, Ruigrok TJ, French P, Jaarsma D, Kistler WM, Meier C, Petrasch-Parwez E, Dermietzel R, Sohl G, Gueldenagel M, Willecke K, Yarom Y (2003) Deformation of network connectivity in the inferior olive of connexin 36-deficient mice is compensated by morphological and electrophysiological changes at the single neuron level. *J Neurosci* 23:4700–4711.
- Eccles JC, Llinás R, Sasaki K (1966) The excitatory synaptic action of climbing fibers on the Purkinje cells of the cerebellum. *J Physiol (Lond)* 182:268–296.
- Fellin T, Pascual O, Gobbo S, Pozzan T, Haydon PG, Carmignoto G (2004) Neuronal synchrony mediated by astrocytic glutamate through activation of extrasynaptic NMDA receptors. *Neuron* 43:729–743.
- Lampl I, Yarom Y (1997) Subthreshold oscillations and resonant behavior: two manifestations of the same mechanism. *Neuroscience* 78:325–341.
- Lang EJ (2001) Organization of olivocerebellar activity in the absence of excitatory glutamatergic input. *J Neurosci* 21:1663–1675.
- Lang EJ (2002) GABAergic and glutamatergic modulation of spontaneous and motor-cortex-evoked complex spike activity. *J Neurophysiol* 87:1993–2008.
- Lang EJ, Sugihara I, Llinás R (1996) GABAergic modulation of complex spike activity by the cerebellar nucleoolivary pathway in rat. *J Neurophysiol* 76:255–275.
- Lang EJ, Sugihara I, Welsh JP, Llinás R (1999) Patterns of spontaneous Purkinje cell complex spike activity in the awake rat. *J Neurosci* 19:2728–2739.
- Leznik E (2004) Spatio-temporal characteristics of oscillatory patterns in the inferior olivary nucleus. PhD thesis, New York University, School of Medicine.
- Leznik E, Llinás R (2003) Role of gap junctions in generating and synchronizing oscillations in the inferior olivary nucleus. *Soc Neurosci Abstr* 29:274.12.
- Leznik E, Llinás R (2005) Role of gap junctions in synchronized neuronal oscillations in the inferior olive. *J Neurophysiol* 94:2447–2456.
- Llinás R (1974) Eighteenth Bowditch lecture. Motor aspects of cerebellar control. *Physiologist* 17:19–46.
- Llinás R, Sasaki K (1989) The functional organization of the olivo-cerebellar system as examined by multiple Purkinje cell recordings. *Eur J Neurosci* 1:587–602.
- Llinás R, Yarom Y (1981a) Electrophysiology of mammalian inferior olivary neurones in vitro. Different types of voltage-dependent ionic conductances. *J Physiol (Lond)* 315:549–567.
- Llinás R, Yarom Y (1981b) Properties and distribution of ionic conductances generating electroresponsiveness of mammalian inferior olivary neurones in vitro. *J Physiol (Lond)* 315:569–584.
- Llinás R, Yarom Y (1986) Oscillatory properties of guinea-pig inferior olivary neurones and their pharmacological modulation: an in vitro study. *J Physiol (Lond)* 376:163–182.
- Llinás R, Baker R, Sotelo C (1974) Electrotonic coupling between neurons in cat inferior olive. *J Neurophysiol* 37:560–571.
- Long MA, Deans MR, Paul DL, Connors BW (2002) Rhythmicity without synchrony in the electrically uncoupled inferior olive. *J Neurosci* 22:10898–10905.
- Manor Y, Rinzel J, Segev I, Yarom Y (1997) Low-amplitude oscillations in the inferior olive: a model based on electrical coupling of neurons with heterogeneous channel densities. *J Neurophysiol* 77:2736–2752.
- Manor Y, Yarom Y, Chorev E, Devor A (2000) To beat or not to beat: a decision taken at the network level. *J Physiol (Paris)* 94:375–390.
- Marshall SP, Willecke K, De Zeeuw CI, Lang EJ (2004) Patterns of cerebellar activity in the normal and connexin 36-knock-out mouse. *Soc Neurosci Abstr* 30:535.19.
- Placantonakis DG, Bukovsky AA, Zeng X-H, Kiem H-P, Welsh JP (2004) Fundamental role of inferior olive connexin 36 in muscle coherence during tremor. *Proc Natl Acad Sci USA* 101:7164–7169.
- Rheinallt Parri H, Gould TM, Crunelli V (2001) Spontaneous astrocytic Ca^{2+} oscillations *in situ* drive NMDAR-mediated neuronal excitation. *Nat Neurosci* 4:803–812.
- Rozental R, Srinivas M, Spray DC (2001) How to close a gap junction channel. In: *Methods in molecular biology*, Vol 154, Connexin methods and protocols (Bruzzone R, Giaume C, eds), pp 447–476. Totowa, NJ: Humana.
- Ruigrok TJH, De Zeeuw CI (1993) Electron microscopy of in vivo recorded and intracellularly injected inferior olivary neurons and their GABAergic innervation in the cat. *Microsc Res Tech* 24:85–102.
- Ruigrok TJH, Voogd J (1995) Cerebellar influence on olivary excitability in the cat. *Eur J Neurosci* 7:679–693.
- Sasaki K, Bower JM, Llinás R (1989) Multiple Purkinje cell recording in rodent cerebellar cortex. *Eur J Neurosci* 1:572–586.
- Snedecor GW, Cochran WG (1989) Statistical methods, Ed 8. Ames, IA: Iowa State UP.
- Sotelo C, Llinás R, Baker R (1974) Structural study of inferior olivary nucleus of the cat: morphological correlates of electrotonic coupling. *J Neurophysiol* 37:541–559.
- Sugihara I, Shinoda Y (2004) Molecular, topographic, and functional organization of the cerebellar cortex: a study with combined aldolase C and olivocerebellar tracing. *J Neurosci* 24:8771–8785.
- Sugihara I, Lang EJ, Llinás R (1993) Uniform olivocerebellar conduction time underlies Purkinje cell complex spike synchronicity in the rat cerebellum. *J Physiol (Lond)* 470:243–271.
- Tare M, Coleman HA, Parkington HC (2002) Glycylrrhethinic derivatives inhibit hyperpolarization in endothelial cells of guinea pig and rat arteries. *Am J Physiol* 282:H335–H341.
- Yamamoto T, Fukuda M, Llinás R (2001) Bilaterally synchronous complex spike Purkinje cell activity in the mammalian cerebellum. *Eur J Neurosci* 13:327–339.
- Yarom Y (1991) Rhythmogenesis in a hybrid system—interconnecting an olivary neuron to an analog network of coupled oscillators. *Neuroscience* 44:263–275.